

# 1 Soil water retention and hydraulic conductivity measured in a wide 2 saturation range

3 Tobias L. Hohenbrink<sup>1,2</sup>, Conrad Jackisch<sup>3,4</sup>, Wolfgang Durner<sup>1</sup>, Kai Germer<sup>1,5</sup>, Sascha C. Iden<sup>1</sup>, Janis  
4 Kreiselmanier<sup>6,7</sup>, Frederic Leuther<sup>8,9</sup>, Johanna C. Metzger<sup>10,11</sup>, Mahyar Naseri<sup>1,5</sup>, Andre Peters<sup>1</sup>

5 <sup>1</sup> Institute of Geocology, Soil Science & Soil Physics, TU Braunschweig, Braunschweig, 38106, Germany

6 <sup>2</sup> Deutscher Wetterdienst (DWD), Agrometeorological Research Center, Braunschweig, 38116, Germany

7 <sup>3</sup> Interdisciplinary Environmental Research Centre, TU Bergakademie Freiberg, Freiberg, 09599, Germany

8 <sup>4</sup> Institute for Water and River Basin Management, Chair of Hydrology, Karlsruhe Institute of Technology (KIT), Karlsruhe,  
9 76131, Germany

10 <sup>5</sup> Thünen Institute of Agricultural Technology, Braunschweig, 38116, Germany

11 <sup>6</sup> Thünen Institute of Forest Ecosystems, Eberswalde, 16225, Germany

12 <sup>7</sup> Institute of Soil Science and Site Ecology, TU Dresden, Tharandt, 01737, Germany

13 <sup>8</sup> Helmholtz Centre for Environmental Research - UFZ, Department of Soil System Sciences, Halle (Saale), 06120, Germany

14 <sup>9</sup> Chair of Soil Physics, University of Bayreuth, 95447 Bayreuth, Germany

15 <sup>10</sup> Institute of Soil Science, Center for Earth System Research and Sustainability (CEN), Universität Hamburg, Hamburg,  
16 20146, Germany

17 <sup>11</sup> Institute of Geoscience, Group of Ecohydrology, Friedrich Schiller University Jena, Jena, 07749, Germany

18  
19  
20 *Correspondence to:* Tobias L. Hohenbrink (t.hohenbrink@tu-braunschweig.de)

21 **Abstract.** Soil hydraulic properties (SHP), particularly soil water retention capacity and hydraulic conductivity of unsaturated  
22 soils, are among the key properties that determine the hydrological functioning of terrestrial systems. Some large collections  
23 of SHP, such as the UNSODA and HYPRES databases, already exist for more than two decades. They have provided an  
24 essential basis for many studies related to the critical zone. Today, sample-based SHP can be determined in a wider saturation  
25 range and with higher resolution by combining some recently developed laboratory methods. We provide 572 high-quality  
26 SHP data sets from undisturbed, mostly central European samples covering a wide range of soil texture, bulk density and  
27 organic carbon content. A consistent and rigorous quality filtering ensures that only trustworthy data sets are included. The  
28 data collection contains: (i) SHP data: soil water retention and hydraulic conductivity data, determined by the evaporation  
29 method and supplemented by retention data obtained by the dew point method and saturated conductivity measurements, (ii)  
30 basic soil data: particle size distribution determined by sedimentation analysis and wet sieving, bulk density and organic carbon  
31 content, as well as (iii) metadata including the coordinates of the sampling locations. In addition, for each data set, we provide  
32 soil hydraulic parameters for the widely used van Genuchten-Mualem model and for the more advanced Peters-Durner-Iden  
33 model. The data were originally collected to develop and test SHP models and associated pedotransfer functions. However,  
34 we expect that they will be very valuable for various other purposes such as simulation studies or correlation analyses of

35 different soil properties to study their causal relationships. The data is available under the DOI link  
36 <https://doi.org/10.5880/fidgeo.2023.012> (Hohenbrink et al., 2023).

## 37 **1 Introduction**

38 A sound understanding of the hydrological functioning of variably saturated soils in the environmental cycles is important for  
39 numerous applications in agronomy, forestry, water management and other disciplines. The hydrological functioning of soils  
40 is controlled by the soil hydraulic properties (SHP), specifically the water retention and hydraulic conductivity characteristics.  
41 SHP models are essential to simulate water dynamics, solute transport and energy transfers in the vadose zone using water  
42 flow and transport equations. Such SHP models are empirical mathematical representations of the highly non-linear soil  
43 hydraulic curves, which are parameterised based on measured SHP data. In order to estimate SHP from more accessible  
44 information, pedotransfer functions relate SHP parameters to basic soil properties like soil texture, bulk density, and organic  
45 carbon content ( $C_{\text{org}}$ ) (Vereecken et al., 2010; Van Looy et al., 2017).

46 Since the early applications of SHP models in hydrological simulations in the 1980s, there is a demand for such parameters  
47 (Carsel and Parrish, 1988). Commonly, they are derived for specific SHP models (Vereecken et al., 2010), which is most often  
48 the van Genuchten-Mualem model (Van Genuchten, 1980; Mualem, 1976). Fitting non-linear SHP models to observed data  
49 and developing pedotransfer functions both require large data collections containing information about SHP measured over a  
50 large range of saturation in samples with various combinations of basic soil properties. Such data collections are commonly  
51 based on individual soil samples from various profiles.

52 Due to methodological restrictions, data for such applications were first limited to few points on the soil water retention curve  
53 using ceramic pressure plate extractors and pressure-controlled hydraulic conductivity (Brooks and Corey, 1964). Since the  
54 late 1990s, different data collections of SHP and associated basic soil properties have been compiled. They formed the basis  
55 to develop various pedotransfer functions. The freely available Unsaturated Soil Hydraulic Database (UNSODA) provided by  
56 the U.S. Department of Agriculture comprises nearly 800 SHP data sets from disturbed and undisturbed samples (Nemes et  
57 al., 2001). It includes measurements of retention and hydraulic conductivity with different coverage of the saturation range as  
58 well as basic soil properties, e.g. information on soil texture or bulk density. UNSODA was an important basis to develop  
59 ROSETTA (Schaap et al., 2001; Zhang and Schaap, 2017), which is the most established pedotransfer function to predict the  
60 parameters of the van Genuchten-Mualem SHP model.

61 Another prominent large collection of retention and hydraulic conductivity data is the database of the Hydraulic Properties of  
62 European Soils (HYPRES) (Wösten et al., 1999) and its further development as the European Hydropedological Data Inventory  
63 (EU- HYDI) (Weynants et al., 2013) which is unfortunately not freely available. There are a few more specific SHP data  
64 collections, e.g. the HYBRAS data describing Brazilian soils (Otoni et al., 2018), and the collection by Schindler and Müller  
65 (2017) which contains only data measured with the evaporation method (Peters and Durner, 2008; Schindler, 1980). Recently,

66 Gupta et al. (2022) gathered published soil water retention data from 2,702 sites, prepared them for use in land surface modeling  
67 and made them openly accessible.

68 The existing databases have undoubtedly supported a large number of hydrological studies leading to important conclusions,  
69 but they still have some limitations and shortcomings. Often, SHP data only cover a small part of the naturally occurring range  
70 of soil saturation. Gupta et al. (2022) emphasised that in many cases the retention data series contain only a few pairs of data  
71 and lack information in the wet region close to full saturation. Measured saturated hydraulic conductivity ( $K_{\text{sat}}$ ) is included in  
72 several data collections, but detailed information about the unsaturated hydraulic conductivity is still rare.

73 It is technically possible to create pedotransfer functions using only retention and  $K_{\text{sat}}$  data (Assouline and Or, 2013) as has  
74 often been done in the past. However, in such cases the shape of the hydraulic conductivity curves is predicted only from the  
75 water retention curve and scaled to match  $K_{\text{sat}}$ . Hence, the absolute position of the conductivity curve is solely determined by  
76 a single  $K_{\text{sat}}$  value, which is strongly influenced by soil structure and macropore connectivity, which are often not recorded nor  
77 assessed at the time of sampling.

78 A serious development and rigorous testing of full-range SHP models always requires measured unsaturated hydraulic  
79 conductivity data. Zhang et al. (2022) showed impressively how fast a supposedly large number of available SHP data sets can  
80 collapse, when they are filtered by predefined data requirements. They initially gathered 19,510 data sets from established data  
81 collections and first narrowed it down to 14,997 data sets describing undisturbed samples. They then extracted 1,801 lab  
82 measured data sets with information about both soil water retention and hydraulic conductivity. Finally, they extracted data  
83 sets with at least six retention and seven conductivity data pairs, each of which contained at least three data pairs close to  
84 saturation at matric heads larger than -20 cm. They ended up with 194 data sets accounting for only 1 % of the initial number.

85 Given the wide variability of naturally occurring soils, many pedotransfer functions are based on data collections that contain  
86 rather limited soil information. Weihermüller et al. (2021) showed that the choice of the pedotransfer function used in a soil  
87 hydrological model can have considerable effects on simulated water fluxes. The artificial neural network behind ROSETTA  
88 has been trained with 2,134 retention curves, 1,306  $K_{\text{sat}}$  values and 235 unsaturated conductivity curves (Schaap et al., 2001;  
89 Zhang and Schaap, 2017). Considering the wide use of ROSETTA with more than 1,860 citations (retrieved from Scopus on  
90 26/08/2023) it becomes apparent that the specific characteristics of only 235 unsaturated hydraulic conductivity data sets have  
91 been propagated into a large number of applications and conclusions. However, pedotransfer functions can only predict the  
92 SHP within the range covered by the training dataset. Furthermore, they tend to reflect the individual characteristics of the  
93 training data, which are most pronounced in case of small databases. To prevent such bottleneck effects, the basis for  
94 pedotransfer applications needs to be further diversified. This requires new and independent, quality-assured SHP data  
95 collections. With advanced measuring techniques becoming standard in many soil physical laboratories, it is now much easier  
96 to obtain experimental SHP data over a wider range of soil moisture and in the desired high quality.

97 In this paper, we present a collection of 572 new data sets of soil properties measured in soil samples (Hohenbrink et al., 2023)  
98 that are independent of existing databases. Each data set contains (i) SHP, and (ii) basic soil properties such as soil texture,  
99 bulk density and  $C_{\text{org}}$ . The SHP data meet high quality requirements since they have been determined by combining state-of-

100 the-art laboratory techniques, i.e. the evaporation method (Peters and Durner, 2008; Schindler, 1980), the dewpoint  
101 potentiometry (Campbell et al., 2007), and separate  $K_{\text{sat}}$  measurements. In addition, each dataset has undergone thorough  
102 quality control. The data collection covers a wide range of soil textures. Soil texture information is provided according to both  
103 the German (Ad-hoc-Arbeitsgruppe Boden, 2005) and the USDA classification systems (USDA, 1999). Within the silt and  
104 sand classes, we also provide the sub-classes “coarse”, “medium” and “fine” according to the German system.  
105 In support of the FAIR principles (Wilkinson et al., 2016), we provide free access to the data for the development of SHP  
106 models and pedotransfer functions. We expect them to be valuable for a variety of purposes such as simulation studies and  
107 statistical analyses of various soil properties.

## 108 **2 Materials and Methods**

### 109 **2.1 Data sources**

110 A community initiative for collecting and sharing consistent SHP data was launched by researchers from the Division of Soil  
111 Science and Soil Physics at TU Braunschweig. Scientists from four other institutions participated by providing data measured  
112 in their laboratories. Most of the data had already been used to answer individual research questions at various research sites  
113 (Jackisch et al., 2017; Kreiselmeier et al., 2019, 2020; Leuther et al., 2019; Jackisch et al., 2020; Germer and Braun, 2019;  
114 Metzger et al., 2021). Some existing but yet unpublished data sets have been reviewed and integrated into the data collection,  
115 too. In addition, we systematically added data from sites with soil characteristics that were missing from the data collection.  
116 Such data were explicitly measured for this data collection.

117 To be included in the data collection, the data sets had to contain soil water retention and hydraulic conductivity data, measured  
118 in the laboratory by the evaporation method, preferably supplemented by dewpoint method data and also measurements of  
119 saturated hydraulic conductivity. The data sets also had to include information about soil texture, and bulk density, and  
120 preferably  $C_{\text{org}}$ . We have aimed to cover the data space of these basic soil properties as completely as possible. Therefore, we  
121 also included data sets that lacked some of the preferred information, when they added new combinations of basic soil  
122 properties to the data collection.

### 123 **2.2 Soil samples**

124 Each data set is based on one undisturbed soil sample taken in situ with a metal cylinder. In 542 cases the sample volume was  
125  $250 \text{ cm}^3$ , while 30 samples had a volume of  $692 \text{ cm}^3$  as indicated in the metadata table of Hohenbrink et al. (2023). For the  
126 measurement of  $C_{\text{org}}$ , soil texture and retention data in the dry range (dewpoint method), disturbed soil (sub)samples were  
127 taken. In 363 cases, exactly one disturbed sample was assigned to each undisturbed sample, either by taking both samples in  
128 close proximity to each other or by taking the disturbed sample directly from the undisturbed sample material after measuring  
129 the SHP. In the other 209 cases, the disturbed sample was taken as mixed material, representative for an entire site with several  
130 undisturbed sampling points. Consequently, in the latter cases the soil variables derived from the aggregated disturbed samples

131 have been assigned to more than one data set (indicated in the metadata table). Information about the positions of the sampling  
132 sites is available for 555 data sets. It has either been measured by GPS or was taken from aerial images after sampling. The  
133 geo-positions are reported with a lateral accuracy of 100 m, which represents the best accuracy class in Gupta et al. (2022).  
134 The sampling depth is reported for 474 samples in the metadata table.

### 135 **2.3 Laboratory measurements**

136 Soil water retention in the wet (defined here as  $pF < 1.8$ ;  $pF = \log_{10}(-h [cm])$ ) and medium (defined here as  $1.8 < pF < 4.2$ )  
137 moisture range and hydraulic conductivity in the medium moisture range were simultaneously determined with the simplified  
138 evaporation method (Peters and Durner, 2008; Schindler, 1980) using the HYPROP device (METER Group, AG, Germany).  
139 The evaporation method provides information related to the drying branches of the SHP curves. The air entry points of the  
140 tensiometer cups were used as an additional measuring point (Schindler et al., 2010) in cases where the duration of the  
141 evaporation experiments was long enough. Soil water retention information was supplemented mainly in the dry moisture  
142 range (defined here as  $pF > 4.2$ ) by measurements with the dewpoint method (Campbell et al., 2007; Kirste et al., 2019) using  
143 the WP4C device (METER Group, Inc., USA). Hydraulic conductivity of the saturated soil was measured in the undisturbed  
144 samples either with the falling head or the constant head method using the KSAT device (METER Group, AG, Germany).  
145 Particle size distributions of the disturbed soil samples were determined by wet sieving for the sand fractions and sedimentation  
146 methods for the silt fractions and clay content (DIN ISO 11277, 2002). The sedimentation analyses were carried out with  
147 slightly different approaches in each lab as specified for each dataset in the metadata table. The respective particle size classes  
148 were defined by the German soil classification system (Ad-hoc-Arbeitsgruppe Boden, 2005). Because the German system  
149 differs from international standards in the boundary between silt and sand (German: 63  $\mu\text{m}$ , USDA: 50  $\mu\text{m}$ ) we additionally  
150 converted the texture data by interpolation with monotone cubic splines fitted to the cumulative particle size distributions as  
151 recommended by Nemes et al. (1999). Illustrations showing data in the texture triangle were created using the “soiltexture” R-  
152 package (Moeys, 2018). Bulk density of each sample was determined by oven-drying for at least 24 h after the evaporation  
153 experiments.  $C_{\text{org}}$  was determined with high-temperature combustion using different elemental analysers, which are listed in  
154 the metadata table.

### 155 **2.4 Data preparation and quality check**

156 The results of all SHP measurements have been compiled with the HYPROP-FIT software (Pertassek et al., 2015). It was  
157 developed to organise and evaluate raw data from the simplified evaporation method, the dewpoint potentiometry and  
158 individual  $K_{\text{sat}}$  measurements.

159 Despite a high level of automation and standardisation, manual adjustments to selecting the raw data for evaluation is required.  
160 To avoid misalignment due to differences in the manual treatment, all resulting retention and hydraulic conductivity points  
161 have been re-checked for plausibility by the same expert based on the following procedure:

- 162 1. Tensiometer check and offset correction: HYPROP uses two tensiometers at different levels. If in the first hours of  
163 the experiments (close to saturation) the measured difference between the upper and lower tensiometers deviate from  
164 the actual difference of 2.5 cm by more than 1 cm, an offset correction was performed to prevent unrealistic hydraulic  
165 gradients during data evaluation.
- 166 2. Consistency check if the initial water content was smaller than the porosity: If not, a slightly larger column height (1  
167 - 4 mm) has been assumed to account for surplus water in the data evaluation.
- 168 3. Setting the evaluation limits of the evaporation method: Because not all measurements follow idealistic conditions,  
169 the data for evaluation have been limited to plausible records (capillary connection of the tensiometers, plausible  
170 upward gradient, omission of scattered values for unsaturated conductivity near saturation).
- 171 4. Omit retention data of the dewpoint potentiometry outside its validity limits: dewpoint potentiometry measurements  
172 tend to be less precise for lower tensions. To avoid unnecessary variance between the different methods (dewpoint  
173 and evaporation), values below pF 4 were omitted.
- 174 5. Plausibility of hydraulic conductivity values: In cases of values for unsaturated conductivity exceeding the separately  
175 measured saturated conductivity, such values were omitted.
- 176 6. Visual alignment check for data from the three methods ( $K_{\text{sat}}$ , evaporation, dewpoint) and omission of obviously  
177 misaligned datasets from the collection.

178 The original binary HYPROP-FIT files are provided by Hohenbrink et al. (2023) to ensure transparency on all manual  
179 adjustments. The final series of measured retention and hydraulic conductivity data were exported from HYPROP-FIT to csv-  
180 files for further data processing, which was mainly performed in R (R Core Team, 2020).

## 181 **2.5 Fitting models to measured SHP data**

182 For direct access to resulting SHP model parameters, we fitted two models to the measured soil water retention and hydraulic  
183 conductivity data using a shuffled complex evolution (Duan et al., 1992) in SHYPFIT 2.0 (Peters and Durner, 2015). The first  
184 model is the well-established van Genuchten-Mualem (VGM) model (Van Genuchten, 1980; Mualem, 1976). The second  
185 model is the recent version of the Peters-Durner-Iden (PDI) model with the VGM model as the basic function (Peters et al.,  
186 2021, 2023).

187 The PDI model specifically considers (i) capillary water in completely filled pores and (ii) non-capillary water in thin films on  
188 particle surfaces and in corners and ducts of the pore system. The explicit consideration of non-capillary water yields more  
189 realistic retention and hydraulic conductivity curves in the medium and dry moisture range. Furthermore, the description of  
190 hydraulic conductivity in the dry range includes an effective component that reflects isothermal vapour flux (Peters, 2013).

191 Retention and conductivity parameters were estimated simultaneously. During model fitting the few retention points measured  
192 with the dewpoint method were weighted ten times higher than those obtained with the evaporation method because the latter  
193 have a much higher abundance. Weights of hydraulic conductivity data were defined in a way that their ratio to the mean  
194 retention data weights was 16 to 10,000 following Peters (2013). We neglected measured  $K_{\text{sat}}$  values in the parameter

195 optimization process, since they mainly reflect effects of soil structure (Weynants et al., 2009), which is not considered in the  
 196 unimodal SHP models. The saturated hydraulic conductivity model parameter  $K_s$  equals the hydraulic conductivity of the  
 197 saturated bulk soil excluding the soil macropore network.

198 For the VGM model six parameters were estimated (residual and saturation water content  $\theta_r$  (-) and  $\theta_s$  (-), the shape parameters  
 199  $\alpha$  ( $\text{cm}^{-1}$ ) and  $n$  (-), the tortuosity parameter  $\lambda$  (-), and the saturated hydraulic conductivity parameter  $K_s$  ( $\text{cm d}^{-1}$ )). The predefined  
 200 parameter limits are listed in Table 1. The upper limits for  $\theta_r$  and  $\theta_s$  were defined as a fraction of porosity  $\Phi$  to ensure physical  
 201 consistency. For the PDI model, five parameters ( $\theta_r$ ,  $\theta_s$ ,  $\alpha$ ,  $n$  and  $\lambda$ ) were estimated with the same settings and fitting algorithms  
 202 as in Peters et al. (2023).

203 Unlike VGM and common models of SHP, where the relative hydraulic conductivity curve is scaled by the saturated  
 204 conductivity  $K_s$ , the new PDI model structure allows to realistically predict conductivity data close to saturation, which are  
 205 usually not available (Peters et al., 2023). To avoid an unrealistically sharp drop of the conductivity curve close to saturation  
 206 for soils with wide pore size distribution, we constrained the conductivity model by a maximum pore radius (maximum tension)  
 207 close to saturation with the “h-clip approach” (Iden et al., 2015). According to Jarvis (2007), the maximum tension was set to  
 208 -6 cm (5 mm equivalent pore diameter). The saturated conductivity is defined as the predicted absolute conductivity at this  
 209 tension. We refer to Peters et al. (2021, 2023) for a more detailed description of the applied version of the PDI model.

210 **Table 1: Upper and lower parameter boundaries for fitting the van Genuchten-Mualem model (VGM) and the Peters-Durner-Iden**  
 211 **model (PDI).  $\alpha$  and  $n$ : shape parameters,  $\theta_r$  and  $\theta_s$ : residual and saturation water content,  $K_s$ : saturated hydraulic conductivity**  
 212 **parameter,  $\lambda$ : tortuosity parameter. Note that the parameter boundaries for  $\theta_r$  and  $\theta_s$  are defined individually as a fraction of the**  
 213 **porosity  $\Phi$ . The boundaries for  $\theta_r$  and  $\lambda$  differ between both models to ensure physical consistency. The lower  $\lambda$  constraint for VGM**  
 214 **is set to guarantee physical consistency while allowing for maximum flexibility.**

	VGM		PDI	
	lower	upper	lower	upper
$\alpha$ ( $\text{cm}^{-1}$ )	$10^{-5}$	0.5	$10^{-5}$	0.5
$n$ (-)	1.01	8.00	1.01	8.00
$\theta_r$ (-)	0.0	$0.25 \cdot \Phi$	0.0	$0.75 \cdot \Phi$
$\theta_s$ (-)	0.2	$\Phi$	0.2	$\Phi$
$K_s$ ( $\text{cm d}^{-1}$ )	$10^{-2}$	$10^5$	-	-

$$\lambda (-) \quad 1 - \frac{2}{1 - \frac{1}{n}} \quad 10 \quad -1 \quad 10$$


---

215

### 216 3 Data description

217 The data collection is structured in the following sections: (i) metadata (file: MetaData.csv), (ii) basic soil properties  
 218 (BasicProp.csv), and (iii) SHP including measured points of the retention curve and hydraulic conductivity curve  
 219 (RetMeas.csv, CondMeas.csv), (iv) optimized parameter sets for two SHP models (Param.csv) and (v) data series resulting  
 220 from both SHP models (HydCurves.csv). Each dataset is labelled by a unique Sample-ID for easy joining of the different  
 221 tables.

#### 222 3.1 Metadata

223 The metadata table summarizes relevant information about the availability of the single variables in each data set. All 572  
 224 datasets contain SHP measurements by the evaporation method, 499 contain at least one dew point measurement and 409 data  
 225 sets include  $K_{sat}$  measurements (Table 2). In 370 data sets all three kinds of SHP information are available. In case of the basic  
 226 soil properties, soil texture and bulk density are available for all datasets and  $C_{org}$  is available in 488 cases. Complete  
 227 information about all variables (SHP and basic soil properties) is contained in 315 data sets (57 %).

228 The data collection contains location information for 555 data sets (see Appendix Figure A1). The sampling sites are not  
 229 arranged systematically, as the region of sampling has not been a criterion for data collection. They are rather clustered in the  
 230 regions where the contributing groups have performed field work. Most of the samples have been taken in Central Europe  
 231 ( $n = 508$ ). Few data sets come from Canada ( $n = 29$ ), Japan ( $n = 5$ ) and Israel ( $n = 30$ ).

232

233 **Table 2: Key variables contained in the data collection, laboratory method used for analyses and number of available samples.**

Measured variable	Laboratory method	Number of available samples
Hydraulic Properties of unsaturated soil	Evaporation method (Peters and Durner, 2008; Schindler, 1980) using the HYPROP device (Pertassek et al., 2015)	572
	Added measurements by air entry point of tensiometer (Schindler et al., 2010)	286



	Added retention measurements by dew point method (Campbell et al., 2007)	499
Hydraulic conductivity of saturated soil	Falling head or constant head method using the KSAT device (METER Group AG, n.d.)	409
Bulk density	Weight of oven dried (105°C) undisturbed samples (Dane and Topp, 2002)	572
Soil texture (63...2000 µm)	Wet sieving with 2000, 630, 200, 63 µm sieves (DIN ISO 11277, 2002)	572
Soil texture (≤ 63 µm)	Pipette method (Köhn, 1931)	300
	Pipette method (Moshrefi, 1993)	78
	Hydrometer method (Dane and Topp, 2002)	52
	Integral suspension pressure method (Durner et al., 2017, Durner and Iden, 2021)	94
	Method unknown	48
Soil organic carbon content	High-temperature combustion using different elemental analysers as listed in the metadata table	488

234

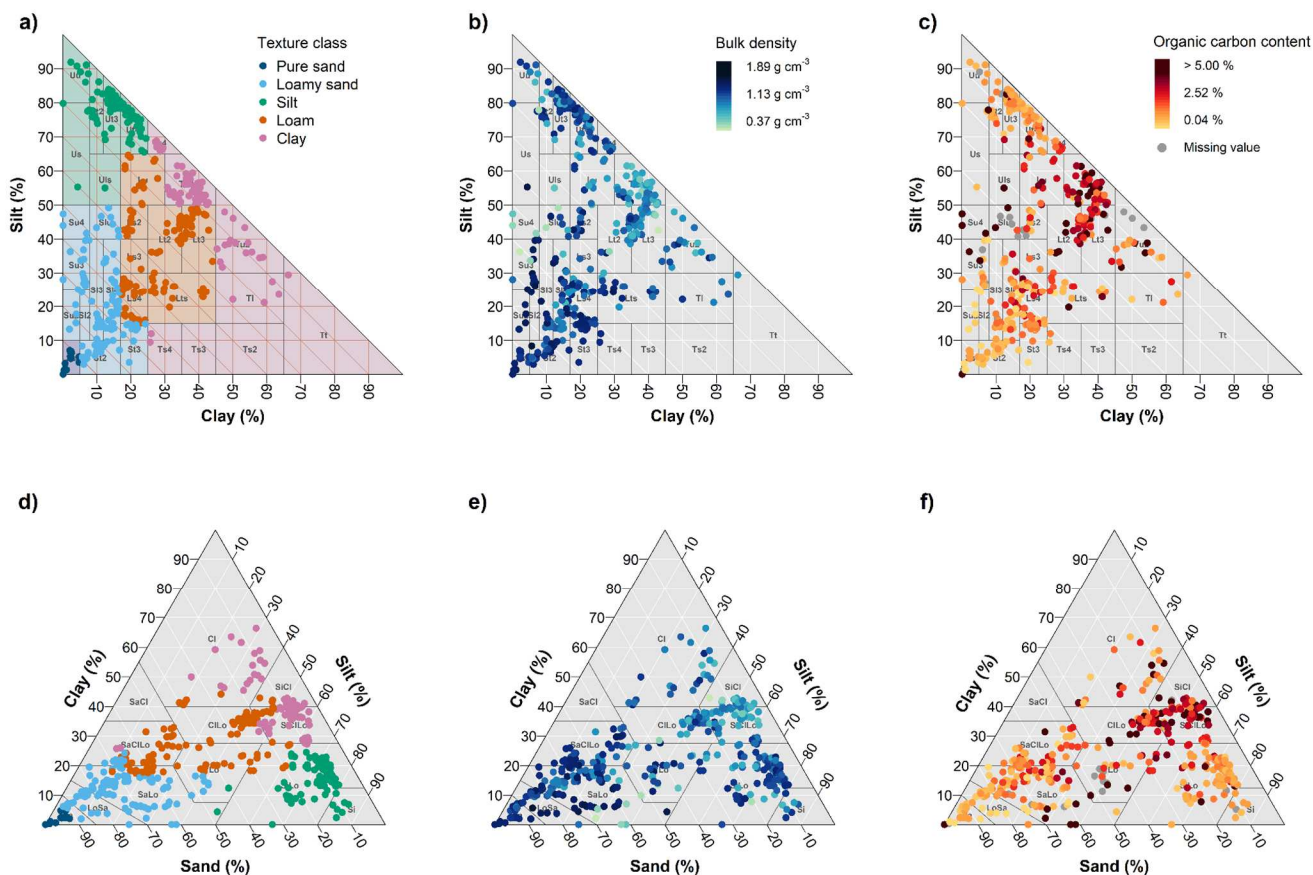
### 235 3.2 Basic soil properties

236 The data collection covers a wide range of soil textures, including soils with up to 65 % clay and 93 % silt and 100 % sand  
237 (positions of symbols in the soil texture triangle, Figure 1). It covers the textures most frequently found in temperate climates.

238 The main textural classes according to the German classification (Ad-hoc-Arbeitsgruppe Boden, 2005) account for 217 (sand),  
239 146 (silt), 121 (loam) and 88 (clay) data sets (Figure 1a). The sandy soils are further subdivided into 39 samples for pure sand  
240 and 178 samples for loamy sand, as the SHP usually have the highest variation within the sand texture class. The two areas in  
241 the soil texture triangle with the lowest data coverage are sandy clay and sandy silt. Figure 1d shows the colour coded samples  
242 in the USDA texture triangle to provide orientation for international readers.

243 The bulk density of the samples varies between 0.37 g cm<sup>-3</sup> and 1.89 g cm<sup>-3</sup> with a median of 1.40 g cm<sup>-3</sup>. High bulk density  
244 mainly occurs in sandy soils while silty clay soils are less dense (Figure 1b and 1e). In general, soil bulk density scatters across  
245 the texture triangle, which is reflected by rather weak but significant Pearson correlations (p-value <0.05) between bulk density  
246 and the sand ( $r = 0.41$ ), silt ( $r = -0.24$ ) and clay ( $r = -0.50$ ) contents, respectively.

247  $C_{org}$  in the samples ranges from 0.04 % to 19.26 % with a median of 1.44 %. The maximum values occur mainly in silty clay,  
 248 loam and silty sand soils. Smaller  $C_{org}$  values are associated with sand and silt soils (Figure 1c and 1f).  
 249 In addition to the standard soil texture classification by sand, silt and clay fractions, the subgroups for silt and sand (i.e. coarse  
 250 sand, medium sand, fine sand, coarse silt, medium silt, and fine silt) are provided for the German classification system (Figure  
 251 2a). Most silt soils contain a maximum fraction of coarse silt (20  $\mu\text{m}$  - 63  $\mu\text{m}$ ), while the loamy sands are mainly dominated  
 252 by the fine sand fraction (63  $\mu\text{m}$  - 200  $\mu\text{m}$ ). In contrast to the weak correlation between soil texture with  $C_{org}$  and bulk density,  
 253 the latter are negatively correlated to each other ( $r=-0.76$ ; Figure 2b).



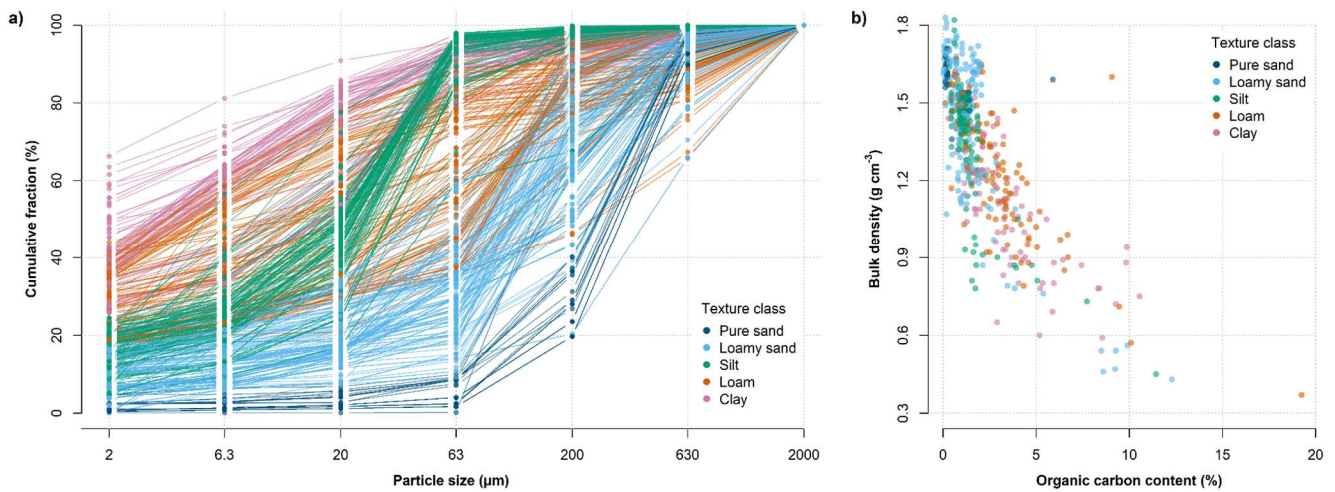
254

255 **Figure 1: Distributions of texture classes (a, d), bulk density (b, e) and organic carbon content (c, f) in the texture triangle of the**  
 256 **German (a-c) and USDA (d-f) system.**

257

258

259



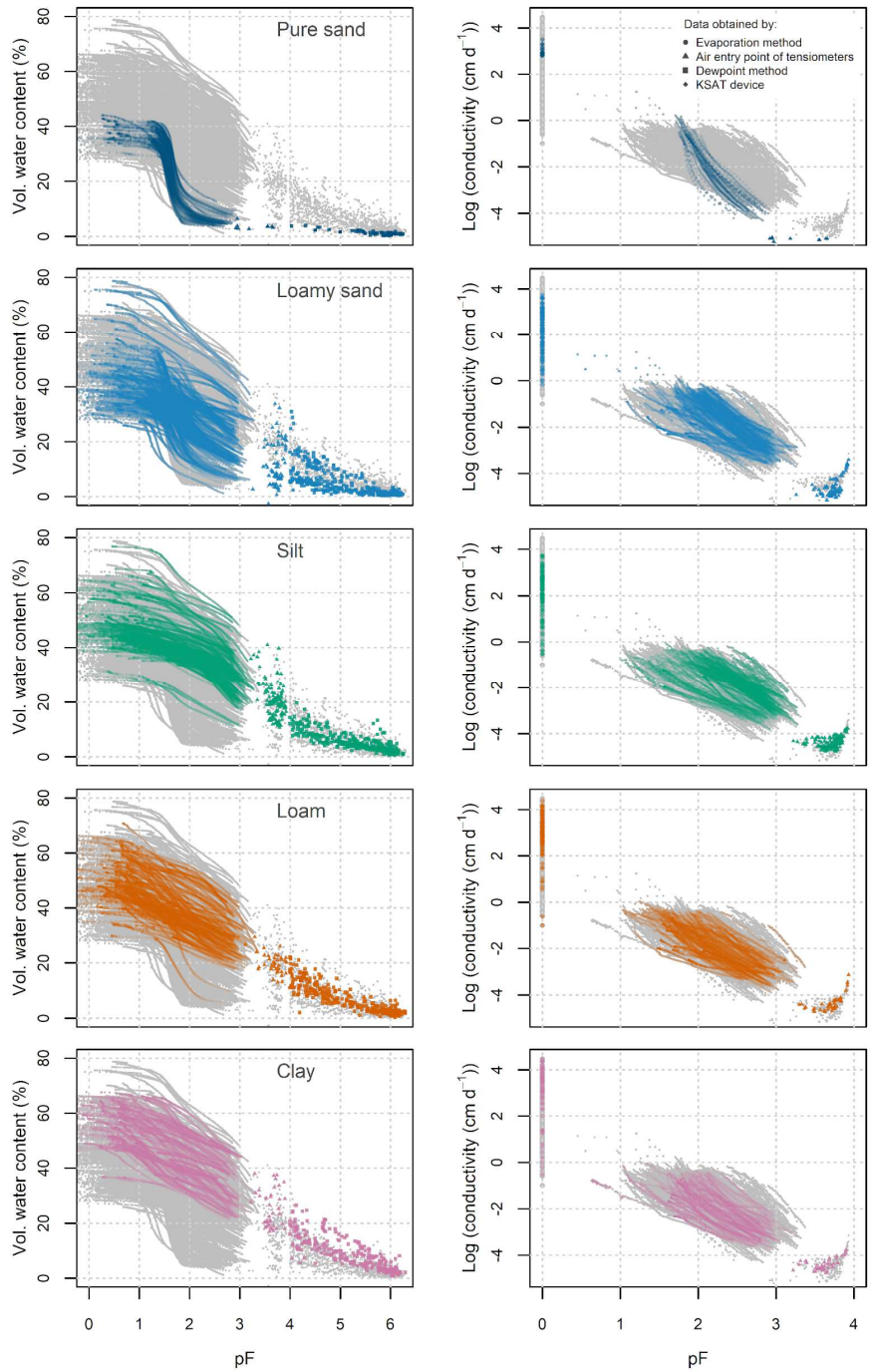
260

261 **Figure 2: a) Cumulative particle size distributions of the 572 samples (German classification system). b) Scatterplot of  $C_{org}$  and bulk**  
 262 **density ( $r=-0.76$ ). The reference texture classes are colour coded.**

### 263 3.3 Measured soil hydraulic data

264 The measured SHP are shown in Figure 3. The retention data cover almost the entire range between full water saturation and  
 265 oven dryness. The highest data coverage is available in the wet and medium saturation range with  $pF < 3.2$ , where the data  
 266 stem from the simplified evaporation method. Half of the datasets contain one additional data point between  $pF 3.0$  and  $pF 4.0$   
 267 which originates from the air entry pressure of the porous tensiometers cup. In 499 data sets at least one data pair between  $pF$   
 268  $4.0$  and  $pF 6.3$  determined by the dewpoint method exists. To cover the drying branch towards  $pF 6.8$  the number of  
 269 measurements for single samples ranges between 1 and 8 (with a median of 3), because this method can only assess the matric  
 270 head values after each reading of the respective sample states.

271 Hydraulic conductivity data obtained by the evaporation method range mostly from  $pF 1.0$  to  $pF 3.2$ . Again, one single  
 272 conductivity data point originates from the air-entry of the porous cup for about half of the datasets. A separately measured  
 273  $K_{sat}$  is available for 409 datasets. The data collection neither contains conductivity data in the range close to saturation ( $pF < 1$ ),  
 274 nor in the dry range. Currently, there is no standard laboratory method to determine hydraulic conductivity in this range. In the  
 275 online version in Figure 3 the different methods contributing to the retention and conductivity data are plotted as circles  
 276 (evaporation), triangles (air entry point), squares (dewpoint) and diamonds ( $K_{sat}$ ). Figure 4 presents the same data colour coded  
 277 by bulk density.



278

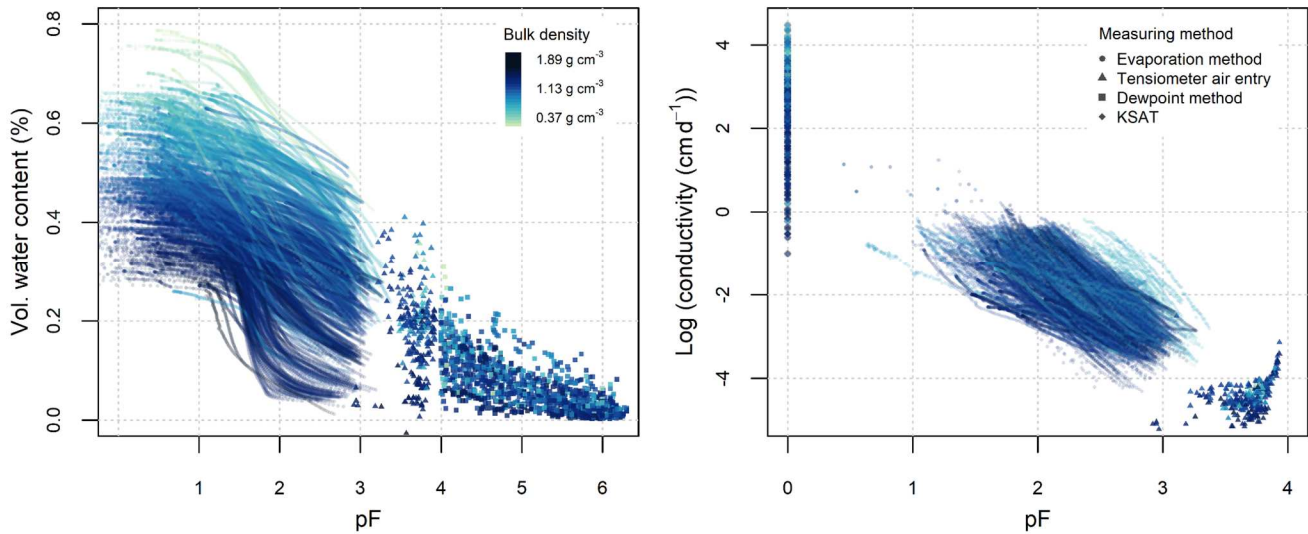
279

280

281

282

**Figure 3: Soil water retention (left) and hydraulic conductivity (right) grouped and colour coded by texture class. Grey background symbols show all measured values. Please note the different pF ranges for the retention and conductivity curves. In the online version the different laboratory methods contributing to the retention and conductivity data are plotted as circles (evaporation), triangles (air entry point), squares (dewpoint) and diamonds ( $K_{sat}$ ) visible after zooming in.**



283  
 284 **Figure 4: Soil water retention (left) and hydraulic conductivity (right) colour coded by bulk density. Please note the different pF**  
 285 **ranges for the retention and conductivity curves. A more detailed version with the used texture classes is in the Appendix Figure A2.**  
 286 **In the online version the different laboratory methods contributing to the retention and conductivity data are plotted as circles**  
 287 **(evaporation), triangles (air entry point), squares (dewpoint) and diamonds ( $K_{\text{sat}}$ ) visible after zooming in.**

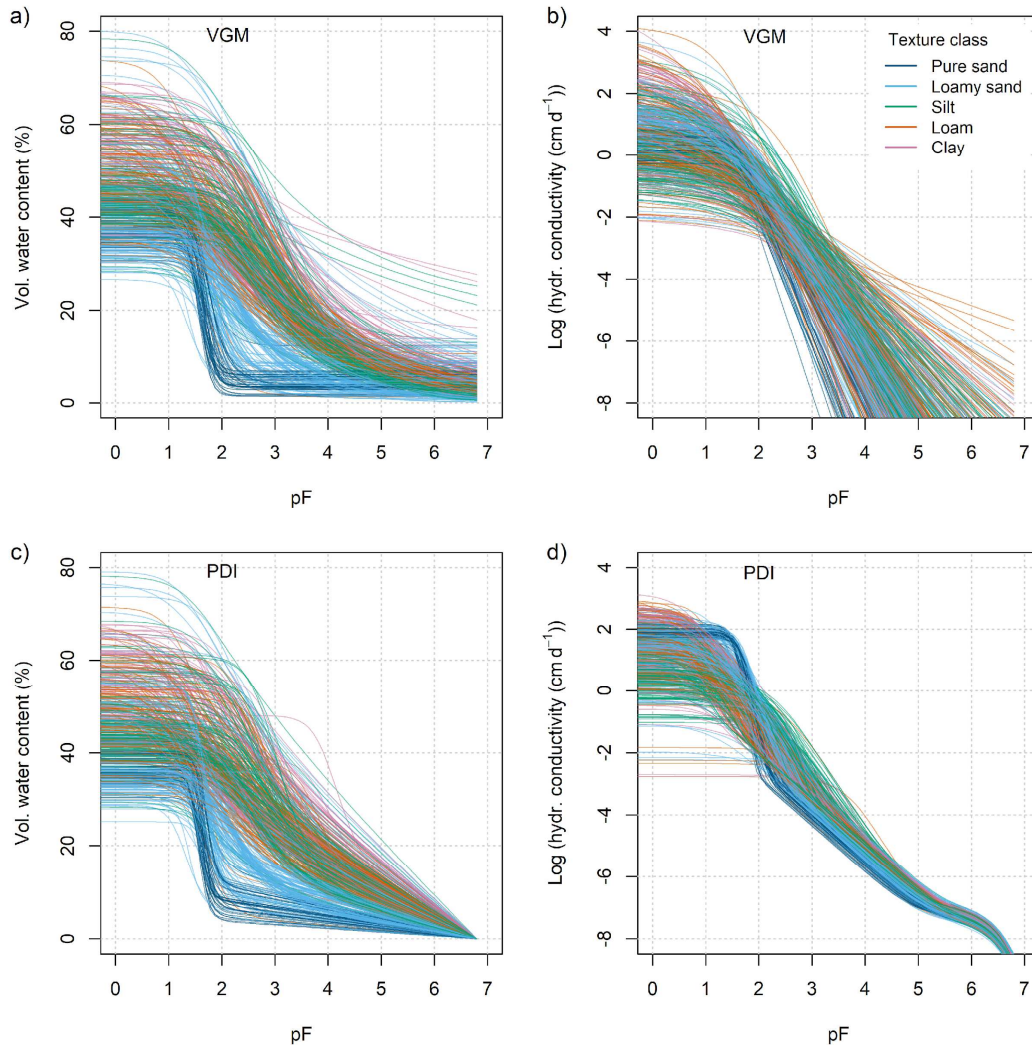
288

### 289 3.4 Fitted SHP models

290 The distributions of the fitted model parameters for both VGM and PDI (data provided in table “Param.csv” in Hohenbrink et  
 291 al. (2023), but not shown here) mostly cover the predefined range of plausible parameters (Table 1). The constraining  
 292 boundaries were only hit in 5 cases except for parameter  $\lambda$  of the PDI model (154 cases in which bounds were hit).

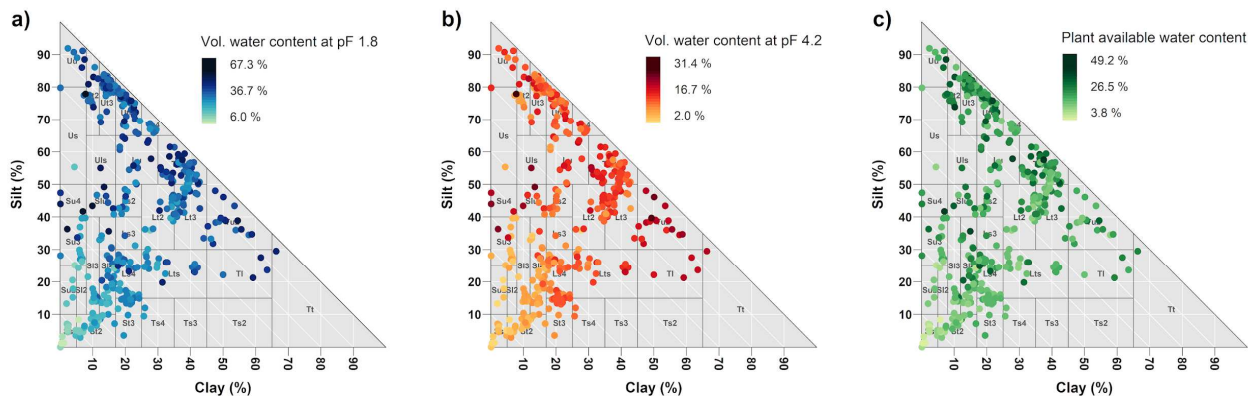
293 The fitted water retention curves (Figure 5a and 5c) reflect the main characteristics of the measured SHP described above.  
 294 Retention curves from both models are similar in the wet to medium range. However, in the medium to dry moisture range  
 295 they systematically differ. The retention curves described by VGM approach a water content between 0% and 28%, while  
 296 those from the PDI model consistently reach zero saturation at  $pF = 6.8$ , which reflects the matric potential at oven dryness  
 297 (Schneider and Goss, 2012). The hydraulic conductivity curves described by VGM (Figure 5b) vary over a wide range. It  
 298 proves difficult to visually relate the curves to respective texture classes, because the wet range part scales strongly with the  
 299 existence of larger pores, and the shape of the curve is strongly limited by the underlying linear fit in log-log space. The PDI  
 300 model curves (Figure 5d) are more closely related to texture and span a much narrower range for each texture class. The  
 301 variation among the curves decreases towards the dry end of the saturation range. Especially in the dry range, the hydraulic  
 302 conductivity increases along the texture gradient from pure sand via loamy sand, silt and loam to clay. This phenomenon  
 303 results from the PDI model structure, where hydraulic conductivity in the dry range is directly derived from the water content  
 304 at  $pF = 5.0$  (Peters et al., 2021). At  $pF > 5.5$  the hydraulic conductivity of the PDI model is dominated by the isothermal  
 305 vapour conductivity for all texture classes.

306 As an estimate for soil water characteristics, we derived soil water content at field capacity ( $\theta$  at  $pF = 1.8$ ), soil water content  
 307 at the permanent wilting point ( $\theta$  at  $pF = 4.2$ ), as well as the resulting plant available water content ( $\theta(pF\ 1.8) - \theta(pF\ 4.2)$ ).  
 308 Figure 6 shows these values in the texture triangle calculated based on the PDI retention curves. The water content at both,  
 309 field capacity (Figure 6a) and wilting point (Figure 6b), roughly increases from sandy soils towards soils with finer textures.  
 310 However, apart from this very general distinction, the values of both variables vary widely over the texture triangle, which  
 311 directly results from the variation of the retention curves within a single texture class (Figure 5c). Plant available water content  
 312 (Figure 6c) depicts the same high variability within the texture triangle. It varies between the extremes of 3.8 vol. % in pure  
 313 sand up to 49.2 vol. % in fine-textured soil but does not align to any clear, texture-related pattern.



314

315 **Figure 5: Retention curves (left, a and c) and hydraulic conductivity curves (right, b and d) for the van Genuchten-Mualem model**  
 316 **(a and b) and the PDI model with VGM basic function (c and d). Soil texture classes are colour coded.**



318

319 **Figure 6: Volumetric water contents at (a) field capacity, (b) the plant wilting point, and (c) the resulting plant available water**  
 320 **scattered on the soil texture triangle. The values provided in the data collection are calculated from retention curves described by**  
 321 **the PDI model.**

## 322 4 Discussion

### 323 4.1 New applications arising from the data collection

324 The combination of different state-of-the-art methods to measure soil water retention and hydraulic conductivity based on  
 325 undisturbed samples yields a unique SHP data collection. Especially, the denser coverage of a wider range of saturation levels  
 326 compared to existing data collections makes it valuable for new applications. For example, the retention data in the dry range  
 327 measured with the dewpoint method represent essential information to develop retention models that overcome the concept of  
 328 a residual water content, which has been shown to be not physically consistent (e.g. Schneider and Goss, 2012; Tuller and Or,  
 329 2005; Nimmo, 1991). Furthermore, this data collection provides measurements of both saturated and unsaturated hydraulic  
 330 conductivity in high resolution and over a wide range of saturation levels. This supports the development and improvement of  
 331 hydraulic conductivity models.

332 The high level of standardisation using the described methods enables us to link data from various labs without methodological  
 333 offsets commonly found due to slightly deviating soil sample processing. Although the data set does not reach any global  
 334 coverage, the data set exceeds existing SHP data collections by data density, extent of the values and variables, and consistency.  
 335 We envision the proposed data structure as a foundation for upcoming additions with the methods becoming more and more  
 336 accessible.

337 The VGM and PDI parameters provided in the data collection have been estimated with state-of-the-art techniques. Both  
 338 parameter sets can be valuable to develop and test simulation models and to perform simulation studies. They can also serve  
 339 as a benchmark for further developments of non-linear parameter estimation algorithms. We have intentionally omitted the  
 340 measured  $K_{sat}$  values during parameter estimation. Considering  $K_{sat}$  in combination with unimodal SHP models usually causes

341 an overestimation of hydraulic conductivity close to saturation since the  $K_{\text{sat}}$  information mainly reflects the impact of soil  
342 structure (Durner, 1994; Peters et al., 2023). The  $K_s$  parameter derived for the PDI can thus be interpreted as the conductivity  
343 of the soil matrix only, excluding effects of soil structure, similarly to Weynants et al. (2009), and as further discussed in  
344 Fatchi et al. (2020). It is now possible to further investigate the relation between  $K_s$  of the soil matrix and  $K_{\text{sat}}$  of the entire soil  
345 including structure effects based on the parameters provided.

346 In addition to the commonly used three fractions sand, silt and clay to classify soil texture, we provide subgroups for sand and  
347 silt. Most pedotransfer functions only consider the three main texture groups as predictor variables. Our data suggests that the  
348 main texture classes alone contain limited information about soil hydraulic properties (large spread of hydraulic curves within  
349 texture classes in Figure 3, scattered texture distribution for plant available water in Figure 6c). Only in combination with bulk  
350 density and  $C_{\text{org}}$ , the data becomes more informative (Figure 4 and A2). For advancing pedotransfer functions, the presented  
351 data collection is a promising basis for analyses of (i) the resolution of texture data and texture class delineation (c.f. Twarakavi  
352 et al., 2010), (ii) the resolution of the SHP data series and (iii) suitable indicators for hydrologic functioning (field capacity,  
353 wilting point, etc. c.f. Assouline and Or, 2014).

#### 354 **4.2 Limitations of the data collection and further research needs**

355 Although the data collection enables many different applications, it has some limitations that must be considered when  
356 analysing the data and interpreting the results. The single data sets are not completely statistically independent from each other  
357 for the following main reasons: (i) many samples stem from identical sites; (ii) some data sets exhibit identical texture and  $C_{\text{org}}$   
358 values, because in these cases only few aggregated disturbed samples representative for a whole site have been taken; (iii) the  
359 analyses have been performed in five different laboratories. However, by closely following the guidelines of the experiments  
360 a high degree of standardisation in the laboratory protocols could be achieved.

361 In some situations, it might be reasonable to thin out the data by keeping only data sets assumed to be statistically independent.  
362 However, whether this is necessary depends on the particular research question and the applied data analysing technique. We  
363 have decided to include all available data sets and to provide enough meta information to evaluate the statistical dependencies  
364 and leave it up to the user to decide how to handle such dependencies.

365 Another limitation of the data that users must cope with is the unbalanced distribution of the datasets in terms of basic soil  
366 properties. For example, Luvisols with silt contents between 70 % and 85 % are overrepresented in the data collection due to  
367 their agricultural importance which led to more frequent soil analyses. In contrast, there are data gaps for the sandy clay and  
368 sandy silt texture classes, because they do occur more sparsely in the regions under study and are generally less intensively  
369 investigated. The unbalanced distribution of the data can be especially challenging for the development of pedotransfer  
370 functions. This problem can be best solved by supplementing the data collection by additional measurements, but this is a  
371 major task at the level of the soil hydrological community and can hardly be achieved by individual researchers.

372 At the level of individual datasets, the gaps in the hydraulic conductivity series near saturation and under dry conditions are  
373 another important limitation. Such data are needed to parameterize existing models in a way that they become more reliable



374 in the respective saturation ranges. More comprehensive hydraulic conductivity data is also required to develop new SHP  
375 models. Therefore, we identify a need for developing and establishing new standard methods to measure hydraulic conductivity  
376 close to saturation (Sarkar et al., 2019b, a) and in the dry range.

### 377 **4.3 Implications for lab procedures and further extension of the data collection**

378 The different texture class definitions required us to estimate the missing breakpoint between USDA sand and silt fractions  
379 based on monotone cubic splines fitted to the German cumulative particle size distributions as recommended by Nemes et al.  
380 (1999). While this technique appears perfectly feasible given the high level of detail in the texture data with seven classes, this  
381 would have been more uncertain when the data would have been limited to the three main texture classes. The estimate can be  
382 eliminated altogether, when the 63  $\mu\text{m}$  sieve and the 50  $\mu\text{m}$  sieve are included as standard.

383 Despite the high level of standardisation using the described techniques to determine SHPs, the quality check based on the  
384 procedure presented in section 2.4 proved to be important to avoid erroneous interpretations and to ensure data quality. When  
385 followed, data from different labs can be easily combined. It would be favourable if this could be extended to further relevant  
386 soil properties e.g. soil texture,  $C_{\text{org}}$ , Mid-Infrared reflection spectra. We encourage the community to use and extend this data  
387 collection.

## 388 **5 Data availability**

389 The data collection is hosted in the repository GFZ Data Services (Hohenbrink et al, 2023). It can be accessed via  
390 <https://doi.org/10.5880/figeo.2023.012>. The rights of use are defined by a creative common licence (CC BY 4.0). The data  
391 collection in the repository includes all data presented in this paper. Further information and materials such as small volumes  
392 of air-dried reserve soil samples can be provided by the corresponding author or the second author (Conrad.Jackisch@tbt.tu-  
393 freiberg.de) upon request.

## 394 **6 Summary and conclusions**

395 Motivated by a need for detailed soil water retention and hydraulic conductivity data, we collected data from 572 undisturbed  
396 ring samples in a community initiative. High level of standardisation in new measurement techniques and rigorous quality  
397 filtering allowed for consistency, which is rarely achieved in soil hydraulic analyses from different labs.

398 Initial comparisons of hydraulic indicators (e.g. plant available water content) with classical texture data showed very weak  
399 predictive power by texture. The addition of more texture classes from the particle size distribution and the addition of  
400 supplementary data on bulk density and organic carbon content appear to be more informative predictors.

401 The data collection can be used in its current form or integrated into existing data collections. All data sets were acquired  
402 directly from the original sources, which makes the data collection completely independent of the existing pool of data on SHP

403 and thus contributes to their diversification. In particular, the hydraulic conductivity series will substantially expand the  
404 existing inventory of SHP data.

405 We expect that this data collection can serve as an independent, new and therefore unexplored benchmark reference to evaluate  
406 already existing SHP models and pedotransfer functions. Due to the high resolution of measured data compared to most data  
407 in existing databases and the extended range of saturation, it is also an ideal basis to develop and test new advanced SHP  
408 models and pedotransfer functions. It is well suited to verify findings and conclusions that have so far emerged from the  
409 existing data collections.

#### 410 **Author contributions**

411 TH compiled and analysed the data, created the figures, and drafted the manuscript in close collaboration with CJ. All co-  
412 authors contributed to the final version. JM, JK, FL, and CJ provided already existing data sets and evaluated them initially.  
413 KG and MN collected samples with new combinations of basic soil properties, performed laboratory measurements, and  
414 evaluated them initially. AP adapted the PDI model and the fitting software, was involved in building the data collection, and  
415 supervised the project. WD and SI supported the data preparation and analyses.

416

#### 417 **Competing Interests**

418 Conrad Jackisch is a member of the editorial board of Earth System Science Data. The authors have no other competing  
419 interests to declare.

#### 420 **Acknowledgements**

421 The initiative of this data collection has emerged from a project funded by the Deutsche Forschungsgemeinschaft (DFG,  
422 German Research Foundation grant PE 1912/4-1). TH and MN were funded by the same project. JM was funded by the  
423 Collaborative Research Centre “AquaDiva”, funded as DFG SFB 1076, project number 218627073. CJ and TH were part of  
424 the DFG research unit “From Catchments as Organised Systems to Models Based on Functional Units” (FOR 1598) funded as  
425 DFG grant ZE 533/9-1. We thank Birgit Walter and Ines Andrae for laboratory analyses of the soil samples taken especially  
426 for this initiative. All authors thankfully acknowledge their respective field and lab support. Without their meticulous work  
427 this data set would not have come into existence.

#### 428 **References**

429 Ad-hoc-Arbeitsgruppe Boden: Bodenkundliche Kartieranleitung: mit 41 Abbildungen, 103 Tabellen und 31 Listen, edited by:  
430 Eckelmann, W., In Kommission: E. Schweizerbart’sche Verlagsbuchhandlung (Nägele und Obermiller), Stuttgart, 2005.

431 Assouline, S. and Or, D.: Conceptual and Parametric Representation of Soil Hydraulic Properties: A Review, VADOSE ZONE  
432 J, 12, <http://doi.org/10.2136/vzj2013.07.0121>, 2013.

- 433 Assouline, S. and Or, D.: The concept of field capacity revisited: Defining intrinsic static and dynamic criteria for soil internal  
434 drainage dynamics, *Water Resources Research*, 50, 4787–4802, <https://doi.org/10.1002/2014wr015475>, 2014.
- 435 Brooks, R. H. and Corey, A. T.: Hydraulic properties of porous media, Colorado State University, Fort Collins, Colorado,  
436 1964.
- 437 Campbell, G. S., Smith, D. M., and Teare, B. L.: Application of a Dew Point Method to Obtain the Soil Water Characteristic,  
438 in: *Experimental unsaturated soil mechanics*, Springer, 71–77, [https://doi.org/10.1007/3-540-69873-6\\_7](https://doi.org/10.1007/3-540-69873-6_7), 2007.
- 439 Carsel, R. F. and Parrish, R. S.: Developing joint probability distributions of soil water retention characteristics, *WATER*  
440 *RESOUR RES*, 24, 755–769, <https://doi.org/10.1029/WR024i005p00755>, 1988.
- 441 Dane, J. H. and Topp G. C. (Eds.): *Methods of Soil Analysis: Part 4 Physical Methods*. John Wiley & Sons.,  
442 <https://doi.org/10.2136/sssabookser5.4>, 2002.
- 443 DIN ISO 11277: Soil quality - Determination of particle size distribution in mineral soil material - Method by sieving and  
444 sedimentation (ISO 11277:1998 + ISO 11277:1998 Corrigendum 1:2002). DIN Deutsches Institut für Normung e. V., 2002.
- 445 Duan, Q., Sorooshian, S., and Gupta, V.: Effective and efficient global optimization for conceptual rainfall-runoff models.  
446 *WATER RESOUR RES*. 28, 1015–1031, <https://doi.org/10.1029/91WR02985>, 1992.
- 447 Durner, W.: Hydraulic conductivity estimation for soils with heterogeneous pore structure, *WATER RESOUR RES*, 30, 211–  
448 223, <https://doi.org/10.1029/93WR02676>, 1994.
- 449 Durner, W. and Iden, S.C.: The improved integral suspension pressure method (ISP+) for precise particle size analysis of soil  
450 and sedimentary materials, *SOIL TILL RES*, 213, 105086, <https://doi.org/10.1016/j.still.2021.105086>, 2021.
- 451 Durner, W., Iden, S.C., von Unold, G.: The integral suspension pressure method (ISP) for precise particle-size analysis by  
452 gravitational sedimentation, *WATER RESOUR RES*, 53, 33–48, <https://doi.org/10.1002/2016WR019830>, 2017.
- 453 Fatichi, S., Or, D., Walko, R., Vereecken, H., Young, M. H., Ghezzehei, T. A., Hengl, T., Kollet, S., Agam, N., and Avissar,  
454 R.: Soil structure is an important omission in Earth System Models, *NAT COMMUN*, 11, 1–11,  
455 <https://doi.org/10.1038/s41467-020-14411-z>, 2020.
- 456 Van Genuchten, M. T.: A Closed-form Equation for Predicting the Hydraulic Conductivity of Unsaturated Soils, *SOIL SCI*  
457 *SOC AM J*, 44, 892–898, <https://doi.org/10.2136/sssaj1980.03615995004400050002x>, 1980.
- 458 Germer, K. and Braun, J.: Multi-step outflow and evaporation experiments—Gaining large undisturbed samples and comparison  
459 of the two methods, *J HYDROL*, 577, 123914, <https://doi.org/10.1016/j.jhydrol.2019.123914>, 2019.
- 460 Gupta, S., Papritz, A., Lehmann, P., Hengl, T., Bonetti, S., and Or, D.: Global Soil Hydraulic Properties dataset based on  
461 legacy site observations and robust parameterization, *Scientific Data*, 9, 1–15, <https://doi.org/10.1038/s41597-022-01481-5>,  
462 2022.
- 463 Hohenbrink, T. L., Jackisch, C., Durner, W., Germer, K., Iden, S. C., Kreiselmeier, J., Leuther, F., Metzger, J. C., Naseri, M.,  
464 Peters, A.: Soil hydraulic characteristics in a wide range of saturation and soil properties. GFZ Data Services.  
465 <https://doi.org/10.5880/figeo.2023.012>, 2023.
- 466 Iden, S. C., Peters, A., and Durner, W.: Improving prediction of hydraulic conductivity by constraining capillary bundle models  
467 to a maximum pore size, *ADV WATER RESOUR*, 85, 86–92, <https://doi.org/10.1016/j.advwatres.2015.09.005>, 2015.

- 468 Jackisch, C., Angermann, L., Allroggen, N., Sprenger, M., Blume, T., Tronicke, J., and Zehe, E.: Form and function in hillslope  
469 hydrology: in situ imaging and characterization of flow-relevant structures, *HYDROL EARTH SYST SC*,  
470 <https://doi.org/10.5194/hess-21-3749-2017>, 2017.
- 471 Jackisch, C., Germer, K., Graeff, T., Andrä, I., Schulz, K., Schiedung, M., Haller-Jans, J., Schneider, J., Jaquemotte, J., Helmer,  
472 P., and others: Soil moisture and matric potential—an open field comparison of sensor systems, *EARTH SYST SCI DATA*, 12,  
473 683–697, <https://doi.org/10.5194/essd-12-683-2020>, 2020.
- 474 Jarvis, N. J.: A review of non-equilibrium water flow and solute transport in soil macropores: principles, controlling factors  
475 and consequences for water quality, *SOIL SCI.*, 58, 523-546, <https://doi.org/10.1111/j.1365-2389.2007.00915.x>, 2007.
- 476 Kirste, B., Iden, S. C., and Durner, W.: Determination of the Soil Water Retention Curve around the Wilting Point: Optimized  
477 Protocol for the Dewpoint Method, *SOIL SCI SOC AM J*, 83, 288–299, <https://doi.org/10.2136/sssaj2018.08.0286>, 2019.
- 478 Köhn, M.: Die mechanische Analyse des Bodens mittels Pipettmethode. *Z PFLANZ BODENKUNDE*, 21 (2), 211–222,  
479 <https://doi.org/10.1002/jpln.19310210206>, 1931.
- 480 Kreiselmeier, J., Chandrasekhar, P., Weninger, T., Schwen, A., Julich, S., Feger, K.-H., and Schwärzel, K.: Quantification of  
481 soil pore dynamics during a winter wheat cropping cycle under different tillage regimes, *SOIL TILL RES*, 192, 222–232,  
482 <https://doi.org/10.1016/j.still.2019.05.014>, 2019.
- 483 Kreiselmeier, J., Chandrasekhar, P., Weninger, T., Schwen, A., Julich, S., Feger, K.-H., and Schwärzel, K.: Temporal  
484 variations of the hydraulic conductivity characteristic under conventional and conservation tillage, *GEODERMA*, 362,  
485 114127, <https://doi.org/10.1016/j.geoderma.2019.114127>, 2020.
- 486 Leuther, F., Schlüter, S., Wallach, R., and Vogel, H.-J.: Structure and hydraulic properties in soils under long-term irrigation  
487 with treated wastewater, *GEODERMA*, 333, 90–98, <https://doi.org/10.1016/j.geoderma.2018.07.015>, 2019.
- 488 Van Looy, K., Bouma, J., Herbst, M., Koestel, J., Minasny, B., Mishra, U., Montzka, C., Nemes, A., Pachepsky, Y. A.,  
489 Padarian, J., and others: Pedotransfer Functions in Earth System Science: Challenges and Perspectives, *REV GEOPHYS*, 55,  
490 1199–1256, <https://doi.org/10.1002/2017RG000581>, 2017.
- 491 Meter Group AG: Operation Manual KSAT, URL: [https://library.metergroup.com/Manuals/UMS/KSAT\\_Manual.pdf](https://library.metergroup.com/Manuals/UMS/KSAT_Manual.pdf)  
492 (retrieved on 16.08.2023), no date.
- 493 Metzger, J. C., Filipzik, J., Michalzik, B., and Hildebrandt, A.: Stemflow Infiltration Hotspots Create Soil Microsites Near  
494 Tree Stems in an Unmanaged Mixed Beech Forest, *FRONT FOR GLOB CHANGE*, 4, 701293,  
495 <https://doi.org/10.3389/ffgc.2021.701293>, 2021.
- 496 Moeys, J.: soiltexture: Functions for Soil Texture Plot, Classification and Transformation. R package version 1.5.1.  
497 <https://CRAN.R-project.org/package=soiltexture>, 2018.
- 498 Moshrefi, N.: A new method of sampling soil suspension for particle-size analysis, *SOIL SCI.*, 155, 245–248,  
499 <https://doi.org/10.1097/00010694-199304000-00002>, 1993.
- 500 Mualem, Y.: A New Model for Predicting the Hydraulic Conductivity of Unsaturated Porous Media, *WATER RESOUR RES*,  
501 12, 513–522, <https://doi.org/10.1029/WR012i003p00513>, 1976.
- 502 Nemes, A., Schaap, M., Leij, F., and Wösten, J.: Description of the unsaturated soil hydraulic database UNSODA version 2.0,  
503 *J HYDROL*, 251, 151–162, [https://doi.org/10.1016/S0022-1694\(01\)00465-6](https://doi.org/10.1016/S0022-1694(01)00465-6), 2001.

504 Nemes, A., Wösten, J. H. M., Lilly, A., Oude Voshaar, J.H.: Evaluation of different procedures to interpolate particle-size  
505 distributions to achieve compatibility within soil databases. *GEODERMA*, 90, 187-202. [https://doi.org/10.1016/S0016-](https://doi.org/10.1016/S0016-7061(99)00014-2)  
506 7061(99)00014-2, 1999.

507 Nimmo, J. R.: Comment on the treatment of residual water content in “A consistent set of parametric models for the two-phase  
508 flow of immiscible fluids in the subsurface” by L. Luckner et al., *WATER RESOUR RES*, 27, 661-662,  
509 <https://doi.org/10.1029/91WR00165>, 1991.

510 Ottoni, M. V., Ottoni Filho, T. B., Schaap, M. G., Lopes-Assad, M. L. R., and Rotunno Filho, O. C.: Hydrophysical Database  
511 for Brazilian Soils (HYBRAS) and Pedotransfer Functions for Water Retention, *VADOSE ZONE J*, 17,  
512 <https://doi.org/10.2136/vzj2017.05.0095>, 2018.

513 Pertassek, T., Peters, A., and Durner, W.: *HYPROP-FIT software user’s manual*, V. 3.0, UMS GmbH, Munich, Germany,  
514 URL: [https://library.metergroup.com/Manuals/UMS/Hyprop\\_Manual.pdf](https://library.metergroup.com/Manuals/UMS/Hyprop_Manual.pdf), (retrieved on 16.08.2023), 2015.

515 Peters, A.: Simple consistent models for water retention and hydraulic conductivity in the complete moisture range, *WATER*  
516 *RESOUR RES*, 49, 6765-6780, <https://doi.org/10.1002/wrcr.20548>, 2013.

517 Peters, A. and Durner, W.: Simplified evaporation method for determining soil hydraulic properties, *J HYDROL*, 356, 147-  
518 162, <https://doi.org/10.1016/j.jhydrol.2008.04.016>, 2008.

519 Peters, A. and Durner, W.: *SHYPPFIT 2.0 User’s Manual*. Research Report. Institut für Ökologie, Technische Universität  
520 Berlin, Germany., 2015.

521 Peters, A., Hohenbrink, T. L., Iden, S. C., and Durner, W.: A Simple Model to Predict Hydraulic Conductivity in Medium to  
522 Dry Soil From the Water Retention Curve, *WATER RESOUR RES*, e2020WR029211,  
523 <https://doi.org/10.1029/2020WR029211>, 2021.

524 Peters, A., Hohenbrink, T. L., Iden, S. C., Genuchten, M. T. van, and Durner, W.: Prediction of the absolute hydraulic  
525 conductivity function from soil water retention data, *HYDROL EARTH SYST SC*, 27, 1565-1582,  
526 <https://doi.org/10.5194/hess-27-1565-2023>, 2023.

527 R Core Team: *R: A Language and Environment for Statistical Computing*, R Foundation for Statistical Computing, Vienna,  
528 Austria. URL <https://www.R-project.org/>, 2020.

529 Sarkar, S., Germer, K., Maity, R., and Durner, W.: Measuring near-saturated hydraulic conductivity of soils by quasi unit-  
530 gradient percolation—1. Theory and numerical analysis, *J PLANT NUTR SOIL SC*, 182, 524-534,  
531 <https://doi.org/10.1002/jpln.201800382>, 2019a.

532 Sarkar, S., Germer, K., Maity, R., and Durner, W.: Measuring near-saturated hydraulic conductivity of soils by quasi unit-  
533 gradient percolation—2. Application of the methodology, *J PLANT NUTR SOIL SC*, 182, 535-540,  
534 <https://doi.org/10.1002/jpln.201800383>, 2019b.

535 Schaap, M. G., Leij, F. J., and Van Genuchten, M. T.: ROSETTA: a computer program for estimating soil hydraulic parameters  
536 with hierarchical pedotransfer functions, *J HYDROL*, 251, 163-176, [https://doi.org/10.1016/S0022-1694\(01\)00466-8](https://doi.org/10.1016/S0022-1694(01)00466-8), 2001.

537 Schindler, U.: Ein Schnellverfahren zur Messung der Wasserleitfähigkeit im teilgesättigten Boden an Stechzylinderproben,  
538 *Arch. Acker- u. Pflanzenbau u. Bodenk.*, Berlin, 24, 1-7, 1980.

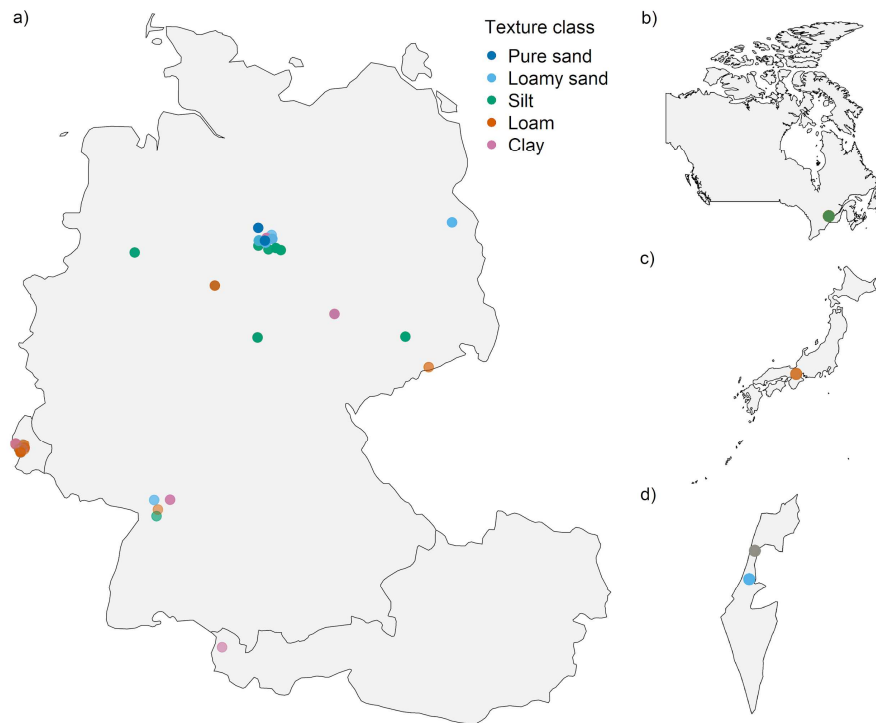
- 539 Schindler, U., Durner, W., Von Unold, G., Mueller, L., and Wieland, R.: The evaporation method: Extending the measurement  
540 range of soil hydraulic properties using the air-entry pressure of the ceramic cup, *J PLANT NUTR SOIL SC*, 173, 563–572,  
541 <https://doi.org/10.1002/jpln.200900201>, 2010.
- 542 Schindler, U. G. and Müller, L.: Soil hydraulic functions of international soils measured with the Extended Evaporation  
543 Method (EEM) and the HYPROP device, *Open Data Journal for Agricultural Research*, 3,  
544 <https://doi.org/10.18174/odjar.v3i1.15763>, 2017.
- 545 Schneider, M. and Goss, K.-U.: Prediction of the water sorption isotherm in air dry soils, *GEODERMA*, 170, 64–69,  
546 <https://doi.org/10.1016/j.geoderma.2011.10.008>, 2012.
- 547 Tuller, M. and Or, D.: Water films and scaling of soil characteristic curves at low water contents, *WATER RESOUR RES*, 41,  
548 <https://doi.org/10.1029/2005WR004142>, 2005.
- 549 Twarakavi, N. K. C., Šimůnek, J., and Schaap, M. G.: Can texture-based classification optimally classify soils with respect to  
550 soil hydraulics?, *Water Resour Res*, 46, <https://doi.org/10.1029/2009wr007939>, 2010.
- 551 USDA: *Soil Taxonomy: A Basic System of Soil Classification for Making and Interpreting Soil Surveys*, 2nd edition, United  
552 States Department of Agriculture, Washington DC, USA, 1999.
- 553 Vereecken, H., Weynants, M., Javaux, M., Pachepsky, Y., Schaap, M., and Genuchten, M. T.: Using Pedotransfer Functions  
554 to Estimate the van Genuchten–Mualem Soil Hydraulic Properties: A Review, *VADOSE ZONE J*, 9, 795–820,  
555 <https://doi.org/10.2136/vzj2010.0045>, 2010.
- 556 Weihermüller, L., Lehmann, P., Herbst, M., Rahmati, M., Verhoef, A., Or, D., Jacques, D., and Vereecken, H.: Choice of  
557 Pedotransfer Functions Matters when Simulating Soil Water Balance Fluxes, *J ADV MODEL EARTH SY*, 13,  
558 e2020MS002404, <https://doi.org/10.1029/2020MS002404>, 2021.
- 559 Weynants, M., Vereecken, H., and Javaux, M.: Revisiting Vereecken Pedotransfer Functions: Introducing a Closed-Form  
560 Hydraulic Model, *VADOSE ZONE J*, 8, 86–95, <https://doi.org/10.2136/vzj2008.0062>, 2009.
- 561 Weynants, M., Montanarella, L., Toth, G., Arnoldussen, A., Anaya Romero, M., Bilas, G., Borresen, T., Cornelis, W.,  
562 Daroussin, J., Gonçalves, M. D. C., and others: European HYdropedological Data Inventory (EU-HYDI), *EUR Scientific and*  
563 *Technical Research Series*, <https://doi.org/10.2788/5936>, 2013.
- 564 Wilkinson, M. D., Dumontier, M., Aalbersberg, I. J., Appleton, G., Axton, M., Baak, A., Blomberg, N., Boiten, J.-W., Silva  
565 Santos, L. B. da, Bourne, P. E., Bouwman, J., Brookes, A. J., Clark, T., Crosas, M., Dillo, I., Dumon, O., Edmunds, S., Evelo,  
566 C. T., Finkers, R., Gonzalez-Beltran, A., Gray, A. J. G., Groth, P., Goble, C., Grethe, J. S., Heringa, J., Hoen, P. A. C. t, Hooft,  
567 R., Kuhn, T., Kok, R., Kok, J., Lusher, S. J., Martone, M. E., Mons, A., Packer, A. L., Persson, B., Rocca-Serra, P., Roos, M.,  
568 Schaik, R. van, Sansone, S.-A., Schultes, E., Sengstag, T., Slater, T., Strawn, G., Swertz, M. A., Thompson, M., Van Der Lei,  
569 J., Van Mulligen, E., Velterop, J., Waagmeester, A., Wittenburg, P., Wolstencroft, K., Zhao, J., and Mons, B.: Comment: The  
570 FAIR Guiding Principles for scientific data management and stewardship, *Scientific Data*, 3,  
571 <https://doi.org/10.1038/sdata.2016.18>, 2016.
- 572 Wösten, J., Lilly, A., Nemes, A., and Le Bas, C.: Development and use of a database of hydraulic properties of European soils,  
573 *GEODERMA*, 90, 169–185, [https://doi.org/10.1016/S0016-7061\(98\)00132-3](https://doi.org/10.1016/S0016-7061(98)00132-3), 1999.
- 574 Zhang, Y. and Schaap, M. G.: Weighted recalibration of the Rosetta pedotransfer model with improved estimates of hydraulic  
575 parameter distributions and summary statistics (Rosetta3), *J HYDROL*, 547, 39–53,  
576 <https://doi.org/10.1016/j.jhydrol.2017.01.004>, 2017.

577 Zhang, Y., Weihermüller, L., Toth, B., Noman, M., and Vereecken, H.: Analyzing dual porosity in soil hydraulic properties  
578 using soil databases for pedotransfer function development, VADOSE ZONE J, e20227, <https://doi.org/10.1002/vzj2.20227>,  
579 2022.

580

## 581 Appendix

582 Since global coverage and regional distribution of the sampling has not been a criterion for data collection, the samples are  
583 basically linked to the research activities of the contributors. Most samples have been taken in Central Europe (n = 508). A  
584 few data sets come from Canada (n = 29), Japan (n = 5) and Israel (n = 30) (Figure A1 for visual reference).  
585

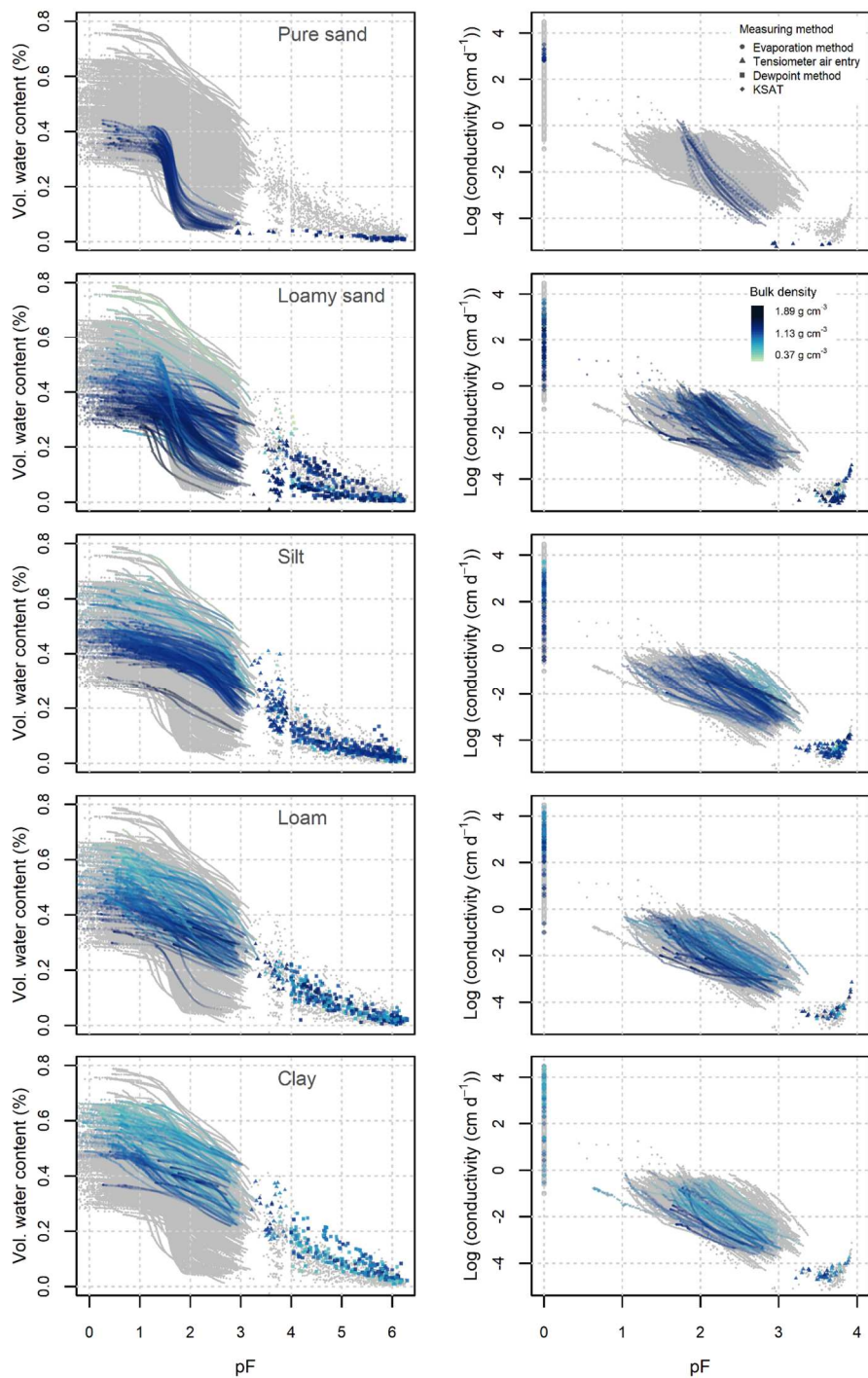


586

587 **Figure A1: Locations of the sampling sites in (a) Luxembourg, Germany and Austria, (b) Canada, (c) Japan, and (d) Israel. Please**  
588 **note that the map scales differ, as the maps should only provide a broad overview.**

589

590 Because soil texture classes did not provide strong information about the soil water retention and hydraulic conductivity curves,  
591 we have added the same plots as in Figure 3 colour-coded by bulk density (Figure A2).



592

593

594

595

**Figure A2: Soil water retention (left) and hydraulic conductivity (right) colour coded by bulk density. Please note the different pF ranges for the retention and conductivity curves. In the online version the different methods contributing to the retention and conductivity data are plotted as circles (evaporation), triangles (air entry point), squares (dewpoint) and diamonds ( $K_{sat}$ ).**